

On-demand Generation of Indistinguishable Photons in the Telecom C-Band using Quantum Dot Devices

Daniel A. Vajner,¹ Paweł Holewa,^{2,3,4} Emilia Zięba-Ostójk,² Maja Wasiluk,² Martin von Helversen,¹ Aurimas Sakanas,³ Alexander Huck,⁵ Kresten Yvind,^{3,4} Niels Gregersen,³ Anna Musiał,² Marcin Syperek,² Elizaveta Semenova,^{3,4} and Tobias Heindel¹

¹*Institute of Solid State Physics, Technical University of Berlin, 10623 Berlin, Germany*

²*Department of Experimental Physics, Faculty of Fundamental Problems of Technology, Wrocław University of Science and Technology, Wyb. Wyspiańskiego 27, 50-370 Wrocław, Poland*

³*DTU Electro, Department of Electrical and Photonics Engineering, Technical University of Denmark, Kongens Lyngby 2800, Denmark*

⁴*NanoPhoton-Center for Nanophotonics, Technical University of Denmark, 2800 Kongens Lyngby, Denmark*

⁵*Center for Macroscopic Quantum States (bigQ), Department of Physics, Technical University of Denmark, 2800 Kgs. Lyngby, Denmark*

(*Electronic mail: tobias.heindel@tu-berlin.de)

(Dated: 16 June 2023)

Semiconductor quantum dots (QDs) enable the generation of single and entangled photons for applications in quantum information and quantum communication. While QDs emitting in the 780nm to 950nm spectral range feature close-to-ideal single-photon purities and indistinguishabilities, they are not the best choice for applications in fiber-optical networks, due to the high optical losses in this wavelength regime. The preferable choice here are QDs operating in the lowest-loss spectral window around 1550 nm (telecom C-band). In this work, we demonstrate the coherent on-demand generation of indistinguishable photons in the telecom C-band from single QD devices consisting of InAs/InP QD-mesa structures heterogeneously integrated with a metallic reflector on a silicon wafer. Using pulsed two-photon resonant excitation of the biexciton-exciton radiative cascade, we observe Rabi rotations up to pulse areas of 4π and a high single-photon purity in terms of $g^{(2)}(0) = 0.005(1)$ and $0.015(1)$ for exciton and biexciton photons, respectively. We obtain two-photon interference visibilities of up to 35(3)% in Hong-Ou-Mandel-type experiments by comparing co- and cross-polarized coincidences. This represents a significant advancement in the photon-indistinguishability of single photons emitted directly in the telecom C-band without wavelength conversion.

I. INTRODUCTION

Single indistinguishable photons are a key resource for many applications in quantum information ranging from quantum communication to distributed quantum computing. They are an essential requirement for quantum networks and the quantum internet¹. While a plethora of quantum emitters enable the generation of single photons^{2,3}, epitaxial semiconductor quantum dots (QD) turned out to be advantageous in many regards⁴⁻⁷. Over the last decades, photons generated on-demand using QDs demonstrated unprecedented quantum optical properties in terms of high purity, brightness and indistinguishability and have been repeatedly employed in implementations of quantum communication⁸. So far, such close-to-ideal single-photon sources have only been demonstrated at wavelengths around 780nm for GaAs/AlGaAs QDs^{9,10} and 930nm for InGaAs/GaAs QDs¹¹⁻¹⁵. For long-distance quantum information transfer via optical fibers, however, wavelengths around 1550nm, i.e. in the telecom C-band, are required to benefit from lowest losses in optical fibers. To shift the emission of QDs to C-band wavelength, quantum frequency conversion of QD-photons emitted at shorter wavelengths can be used¹⁶⁻¹⁸, which introduces additional conversion losses ultimately limiting the source efficiency. For this reason, QDs directly emitting photons at telecom wavelengths are desirable, requiring carefully tailored growth schemes.

One solution is to introduce metamorphic buffer layers to engineer the strain and size of InAs/InGaAs QDs, which shifts the emission to longer wavelengths^{19,20}. QDs grown on metamorphic buffers have been advanced in recent years²¹⁻²³ and recently triggered photon-indistinguishabilities of $V \approx 10\%$ and $V = 14(2)\%$ were reported under quasi-resonant²⁴ and resonant²⁵ excitation, respectively. An alternative approach uses the InP material system for the growth of InAs/InP QDs naturally emitting at telecom C-band wavelengths. Various studies investigated the properties of InP-based QDs under above-band and quasi-resonant excitation²⁶⁻³³. A notable recent advancement in this context concerns the demonstration of a scalable device platform, by deterministically integrating single InAs/InP QDs into circular Bragg grating cavities, resulting in a triggered, Purcell-enhanced emission and a photon-indistinguishability of $V = 19(3)\%$ under quasi-resonant excitation³⁴. The pulsed on-demand generation of InP-based QD single photons at C-band wavelengths, however, is an important requirement for applications that has not been achieved to date.

This work, presents studies on single InAs/InP QDs integrated into mesa structures using pulsed coherent excitation. Coherently driving the biexciton-exciton (XX-X) radiative cascade via triggered two-photon-resonant excitation (TPE) of the XX-state, we demonstrate the on-demand generation of single-photons with high purity in terms of $g^{(2)}(0) \approx 1\%$

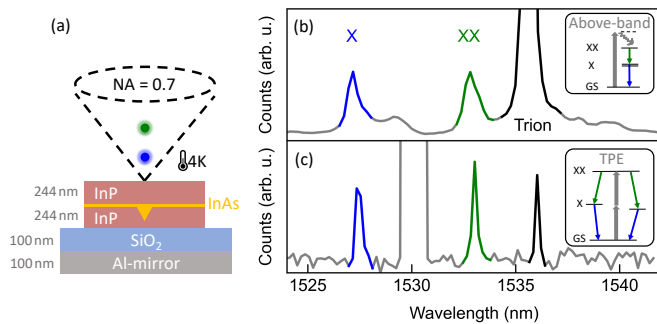


FIG. 1. (a) Illustration of the Si-compatible QD-mesa structure used in this study: a single InAs QD is embedded in an InP matrix with metallic bottom mirror for enhanced photon extraction efficiency. The mesa diameter is $2\mu\text{m}$. (b) Spectrum of a QD-mesa under above-band excitation at saturation power revealing telecom C-band photons originating from the X- (blue), XX- (green) and trion- (black) state, respectively. (c) Spectrum of the same QD under two-photon resonant excitation. Insets illustrate the excitation scheme used. All spectra are taken at 4K, the sample is placed in a closed-cycle cryostat (Attocube) and the emission is collected with an NA = 0.7 aspheric lens.

and record-high photon-indistinguishabilities of 35(3)% in the telecom C-band. Our work thus represents a notable advancement in the generation of flying qubits for quantum networking in optical fibers.

The InAs/InP QDs used in this work have been obtained by self-assembled Stranski-Krastanow growth in the near-critical regime via metalorganic vapor phase epitaxy (MOVPE)³⁵. A bottom metallic mirror (Aluminum) in combination with a top mesa structure enhances the photon extraction efficiency to $\approx 10\%$ ³³, while the silicon (Si) substrate allows future CMOS integration (see Fig. 1(a)). For more information on the device fabrication and a detailed pre-characterization we refer the interested reader to Ref. 33. The spectrum of a single QD-mesa under above-band excitation (continuous wave (CW) laser at 980 nm) is shown in Fig. 1(b). Photons originating from the XX-X radiative cascade and a trion-state of the same QD are observed with wavelengths near 1530 nm in the telecom C-band. The spectral separation of the XX- and X- emission (i.e. the XX binding energy) is determined to be 3.0(1) meV, allowing for TPE of the biexciton state³⁶. Figure 1(c) depicts a spectrum of the same QD from (b) under pulsed TPE, revealing the same spectral fingerprint of the QD together with scattered laser light at 1530 nm. Here, we used laser pulses with a spectral width of $\approx 0.5\text{nm}$ full-width half-maximum (FWHM) (i.e. 10ps pulse duration) sliced from 2ps laser pulses (picoEmerald, APE GmbH) using a 4f pulse-shaper. We extract upper bounds for the linewidths of 180(17) μeV and 120(22) μeV FWHM for the X- and XX-transition, respectively, limited by the spectrometer resolution.

The coherent population of the XX-X cascade under TPE can be confirmed via excitation-power dependent measurements. Figure 2(a) and (b) display the laser-power-dependent integrated emission intensities of the X- and XX-state, respectively. Here, clear Rabi rotations are observed up to pulse areas of 4π accompanied by a noticeable damping ef-

fect. Note that, unlike for strictly resonant excitation, the Rabi frequency scales quadratically with the pulse area under TPE, resulting in equidistant Rabi oscillations as a function of the laser power. Note also that in the presence of damping the pulse area that leads to a complete state occupation inversion (the theoretical π -power) slightly deviates from the power that leads to a maximum in the emission. However, we denote the maximum of the measured Rabi rotation as π -power for simplicity. To estimate a lower bound of the preparation fidelity, we fit an exponentially damped \sin^2 -function to our experimental data³⁷. Extrapolating the envelope function of the oscillations (red dashed line) yields an estimated preparation fidelity, i.e. normalized occupation at π -power, of $\mathcal{F}_{\text{Prep.}} \approx 70\%$. The observed preparation fidelity compares favorably or is comparable with previously reported values between 49% and 85% for QDs at C-band wavelength based on metamorphic buffer layers^{22,38}.

All experiments presented in the following were conducted under TPE with a π -pulse corresponding to $P_{\pi} = 11\mu\text{W}$ average excitation power on the sample. Photons originating from the X- or XX-state were collected via an NA = 0.7 aspheric lens, spectrally filtered using a tunable fiber-bandpass filter of 0.4nm bandwidth in combination with polarization suppression of the scattered excitation laser. Time-correlated single-photon counting experiments were performed using a superconducting nano-wire single-photon detector (SNSPD) system (SingleQuantum EOS by SingleQuantum BV) in combination with time-tagging electronics (quTag by quTools GmbH) with a combined timing resolution of $\approx 50\text{ps}$ FWHM.

To gain insight into the dynamics of the three-level system under study, we conducted time-resolved measurements (see Fig. 2(c)). We observe the typical behavior of the XX-X emission cascade. A fast exponential decay of the XX-state causes the X state to be transiently occupied, followed by a slower exponential decay of the X-state. Applying mono-exponential fits to the time-traces, we extract the respective decay constants as

$$t_{1,X} = 1.279(9)\text{ ns}, \quad t_{1,XX} = 0.333(5)\text{ ns}.$$

Interestingly, the decay of the XX-state is about 4-times faster than the decay of the X-state, which indicates the presence of dark states with short spin-flip times³⁹. Investigating a larger number of quantum emitters, we find that this behavior is representative for the QD ensemble on this sample. Noteworthy, for photons generated via TPE, the indistinguishability is intrinsically limited by the ratio of the XX- and X-lifetime as $V_{\text{max TPE}} = 1/(1 + t_{1,XX}/t_{1,X})$ ⁴⁰. This results in a theoretical limit of $\approx 80\%$ in our case, which significantly exceeds the value of 67% following from the naive expectation of $t_{1,X} = 2 \times t_{1,XX}$. The intuitive explanation for the improved maximum indistinguishability is that a relatively short XX decay time reduces the timing jitter inherited by the X photon. Thus, QDs that display a larger $t_{1,X}/t_{1,XX}$ ratio are promising candidates for combining entanglement generation with high indistinguishability. Technologically more involved approaches in this direction aim to exploit microcavities supporting an asymmetric Purcell enhancement for maximizing this lifetime-ratio⁴¹.

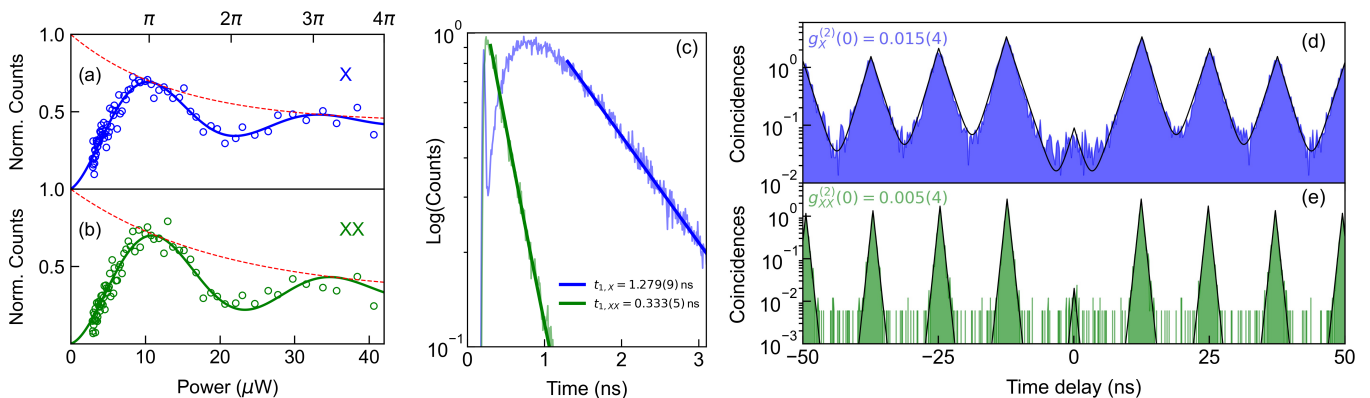


FIG. 2. (a,b) Tuning the excitation laser power reveals Rabi rotations in the emission of X (blue, upper panel) and XX (green, lower panel) up to 4π , confirming the coherent population of the three-level system. Solid lines correspond to fits and red dashed lines to the extracted enveloping function. (c) The decay dynamics illustrate the cascaded emission under pulsed TPE, with the X-photons (blue line) appearing delayed with respect to the XX-photons (green). The XX-state decays ≈ 4 -times faster than the X-state. (d,e) The second-order auto-correlation measurement confirms the single-photon-nature of X- (blue) and XX- (green) photons.

Next, we investigated the purity of the single photons in terms of the second-order auto-correlation function $g^{(2)}(\tau)$ via Hanbury-Brown and Twiss type experiments. The resulting $g^{(2)}(\tau)$ -histograms for X- and XX-photons are depicted in Fig. 2(d) and (e), respectively. The strong suppression of coincidences at zero time delay confirms the emission of single photons. The experimental data are approximated by a fit function corresponding to a sum of two-sided exponential decays and accounting for the noticeable blinking effect on short timescales (following Ref. 34), while no temporal deconvolution or background subtraction was applied. The fit yields antibunching values of

$$g_X^{(2)}(0) = 0.015(4), \quad g_{XX}^{(2)}(0) = 0.005(4)$$

where the errors have been determined from the quality of the fit. The decay times obtained from the fit are 1.44(1) ns and 0.36(1) ns for the X- and XX-state, respectively, in good agreement with the time-resolved photoluminescence measurements. We further extract the timescale of the blinking as $\tau_{\text{blink}} \approx 17(1)$ ns, which can be caused by either charging events or spectral wandering due to fluctuation in the QD's charge environment.

Finally, we explored the photon-indistinguishability of the coherently driven three-level system by means of Hong-Ou-Mandel (HOM) type two-photon interference experiments⁴². For this purpose, XX photons were interfered in an unbalanced Mach-Zehnder interferometer with 12.5 ns delay with one input and two outputs. Here, indistinguishable photons cause coalescence in the two outputs ports, thus reducing the number of detected coincidences. Additionally, the polarization-state of the interfering photons is controlled in both arms of the interferometer, allowing for measurements in co- and cross-polarised configuration, whereas the latter serves as a reference to extract the two-photon-interference visibility V .

The resulting experimental data for the co- and cross-polarized measurement configuration are presented in Fig. 3

as a close-up highlighting the zero-delay peak together with fits (solid lines) following Ref.³⁴ and accounting for the blinking effect. The reduction of coincidences due to two-photon interference is clearly visible. Additionally, the inset depicts the histograms for larger arrival time delays. Note, that the ratios of the coincidence side-peak areas are masked by the blinking effect compared to the expected behavior. This however does not affect the following analysis, which is solely based on the measured coincidences of the zero-delay peak areas for co- and cross-polarized measurements (without applying the fit model).

The two-photon interference visibility is extracted from our measurement data via $V = 1 - (A_{\text{co}}/A_{\text{cross}})$, with the integrated areas A_{co} and A_{cross} of the co- and cross-polarized

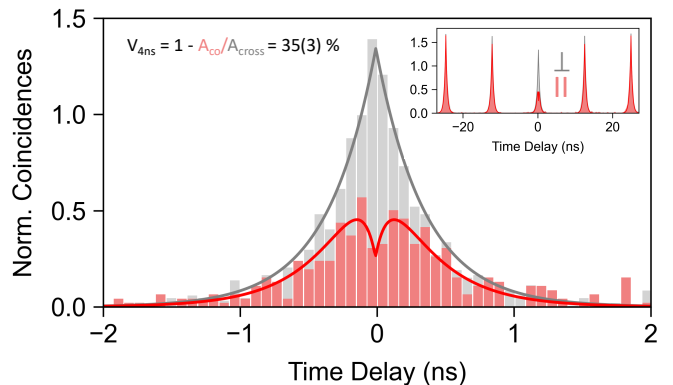


FIG. 3. HOM-type two-photon interference experiments of photons emitted by the XX-state for co- (red) and cross- (grey) polarized measurement configuration. Photon coalescence described by the Hong-Ou-Mandel effect is confirmed by the clear suppression of coincidences in the central peak for co-polarized photons. We observe record-high photon-indistinguishabilities of $V_{\text{raw}} = 29(2)\%$ and $V_{4\text{ns}} = 35(3)\%$ by integrating the raw experimental data over the full 12.5 ns- and a 4 ns-wide delay-window, respectively. The inset shows the same data for a larger range of arrival time delays.

case, respectively. Integrating over the entire zero-delay time window, i.e. -6.25 to $+6.25$ ns (corresponding to the laser repetition rate of 80 MHz), yields $V_{\text{raw}} = 29(2)\%$, with the error inferred from the distribution of the integrated detection events of the non-interfering side-peaks. This photon-indistinguishability readily exceeds all previous reports on pulsed HOM experiments of telecom C-band photons directly generated via QDs (cf. Table I), including pioneering work by Nawrath et al.^{24,25} as well as our most recent work in Ref. 34.

TABLE I. Comparison of achieved pulsed two-photon-interference visibilities for single photons emitted by QDs in the telecom C-Band. MB: Metamorphic Buffer, ES: Excitation Scheme (R: Resonant, QR: Quasi-Resonant, TPE: Two-Photon-Resonant), CBG: Circular Bragg grating. The subscript of the visibility V refers to the coincidence integration window when evaluating the HOM measurement.

QD Type	Device	ES	Visibility	Ref.
InGaAs/InAs + MB	CBG	QR	$V_{6\text{ns}} \approx 10\%$	Ref. ²⁴
InGaAs/InAs + MB	planar	R	$V_{4\text{ns}} = 14(2)\%$	Ref. ²⁵
InAs/InP	CBG	QR	$V_{4\text{ns}} = 19(3)\%$	Ref. ³⁴
InAs/InP	mesa	TPE	$V_{\text{raw}} = 29(2)\%$	This work
InAs/InP	mesa	TPE	$V_{4\text{ns}} = 35(3)\%$	This work

Note, that in these earlier reports, photons with a temporal separation of mostly 4 ns were interfered. Thus, for the sake of comparison, we also evaluate the two-photon interference visibility for a 4 ns-wide integration-window as $V_{4\text{ns}} = 35(1)\%$. Importantly, this analysis still covers more than 99% of all coincidences detected in the zero-delay peak. Thus, the increase in V is a result of the improved signal-to-noise ratio (due to reduced noise contributions by dark counts) rather than discarding signal events. In addition, by interfering photons with a temporal separation of 12.5 ns, the QD-excitonic states investigated in our work are potentially subject to larger dephasing compared to previous studies that used $\Delta t = 4\text{ns}$ ⁴³. While the photon-indistinguishability observed in our work represents a substantial improvement compared to previous reports on QD photons emitted directly at C-band wavelengths, it is not yet competitive with upconverted photons from QDs emitting at lower wavelengths^{17,18}. Further improvements in the photon-indistinguishability are expected by implementing charge control or stabilization via electrical gates.

The triggered on-demand generation of indistinguishable photons at telecom C-band wavelength via TPE achieved in our work represents an important advancement towards applications of quantum information covering large distances in optical fibers. Yet, for implementations of single-photon-based quantum communication, the most suitable excitation scheme needs to be selected depending on the specific use-case. For defining time-bin qubits and synchronizing sender and receiver units, pulsed excitation is needed, while coherent excitation provides the highest indistinguishability. Among all known approaches for pumping QD emitters, coherently driving the XX-X cascade via TPE promises the highest purity in terms of $g^{(2)}(0)$, as it reduces the re-excitation probability¹³. In addition, the spectrally detuned excitation laser allows for straightforward spectral filtering of the emit-

ted photons and for the generation of polarization-entangled photon-pairs⁴⁴. While the maximum indistinguishability is limited in standard TPE⁴⁰, it can be further boosted by stimulating the XX-decay channel to distill highly indistinguishable X-photon⁴⁵⁻⁴⁷.

Another important aspect in quantum communication is whether the emitted photon forms a pure or a mixed state in the photon number basis, which strongly depends on the excitation scheme⁴⁸. For most quantum communication protocols the absence of photon number coherence (PNC) is required to avoid side-channel attacks and maintain security. As recently demonstrated for QD-generated photons at shorter wavelengths, standard TPE does not result in a significant degree of PNC in the emitted photon states, which can however be recovered and tuned by stimulating the XX-decay channel with a second laser pulse⁴⁹.

II. CONCLUSION

In summary, we demonstrated the pulsed coherent excitation of InAs/InP QDs emitting photons at telecom C-band wavelengths. Using triggered TPE of the XX-X radiative cascade, we coherently populate the three-level system, which is confirmed by the observation of Rabi rotations up to 4π . The observed two-photon-interference visibility of up to 35(3)% clearly surpasses previous results obtained for triggered photons in the telecom C-band directly emitted by QDs. The type of QD studied in our work exhibits a large ratio of exciton-to-biexciton lifetime, making them promising candidates for the generation of polarization-entangled photon-pairs with high photon-indistinguishability at C-band wavelength. The demonstrated on-demand generation of QD photons with record-high indistinguishability at wavelengths compatible with existing fiber infrastructure presents a significant step towards scalable quantum networks.

ACKNOWLEDGMENTS

The authors gratefully acknowledge helpful discussions and technical support by Yusuf Karli, Florian Kappe, Thomas Bracht, and Doris Reiter. We further acknowledge financial support by the German Federal Ministry of Education and Research (BMBF) via the project ‘‘QuSecure’’ (Grant No. 13N14876) within the funding program Photonic Research Germany, the BMBF joint project ‘‘tubLAN Q.0’’ (Grant No. 16KISQ087K), the Einstein Foundation via the Einstein Research Unit ‘‘Quantum Devices’’, the Danish National Research Foundation via the Research Centers of Excellence NanoPhoton (DNRF147) and the Center for Macroscopic Quantum States bigQ (DNRF142). P. H. was funded by the Polish National Science Center within the Etiuda 8 scholarship (Grant No. 2020/36/T/ST5/00511). N. G. acknowledges support from the European Research Council (ERC-CoG ‘‘UNITY’’, Grant No. 865230), and from the Independent Research Fund Denmark (Grant No. DFF-9041-00046B).

DATA AVAILABILITY STATEMENT

The data that support the plots within this paper and other findings of this study are available from the corresponding author upon reasonable request.

III. REFERENCES

- ¹H. J. Kimble, *Nature* **453**, 1023 (2008).
- ²I. Aharonovich, D. Englund, and M. Toth, *Nature photonics* **10**, 631 (2016).
- ³C. Chakraborty, N. Vamivakas, and D. Englund, *Nanophotonics* **8**, 2017 (2019).
- ⁴P. Senellart, G. Solomon, and A. White, *Nature nanotechnology* **12**, 1026 (2017).
- ⁵Y. Arakawa and M. J. Holmes, *Applied Physics Reviews* **7**, 021309 (2020).
- ⁶S. Rodt, S. Reitzenstein, and T. Heindel, *Journal of Physics: Condensed Matter* **32**, 153003 (2020).
- ⁷C.-Y. Lu and J.-W. Pan, *Nature Nanotechnology* **16**, 1294 (2021).
- ⁸D. A. Vajner, L. Rickert, T. Gao, K. Kaymazlar, and T. Heindel, *Advanced Quantum Technologies* **5**, 2100116 (2022).
- ⁹L. Schweickert, K. D. Jöns, K. D. Zeuner, S. F. Covre da Silva, H. Huang, T. Lettner, M. Reindl, J. Zichi, R. Trotta, A. Rastelli, *et al.*, *Applied Physics Letters* **112**, 093106 (2018).
- ¹⁰E. Schöll, L. Hanschke, L. Schweickert, K. D. Zeuner, M. Reindl, S. F. Covre da Silva, T. Lettner, R. Trotta, J. J. Finley, K. Müller, *et al.*, *Nano Letters* **19**, 2404 (2019).
- ¹¹O. Gazzano, S. Michaelis de Vasconcellos, C. Arnold, A. Nowak, E. Galopin, I. Sagnes, L. Lanco, A. Lemaître, and P. Senellart, *Nature communications* **4**, 1425 (2013).
- ¹²H. Wang, Z.-C. Duan, Y.-H. Li, S. Chen, J.-P. Li, Y.-M. He, M.-C. Chen, Y. He, X. Ding, C.-Z. Peng, *et al.*, *Physical Review Letters* **116**, 213601 (2016).
- ¹³L. Hanschke, K. A. Fischer, S. Appel, D. Lukin, J. Wierzbowski, S. Sun, R. Trivedi, J. Vučković, J. J. Finley, and K. Müller, *npj Quantum Information* **4**, 43 (2018).
- ¹⁴R. Uppu, F. T. Pedersen, Y. Wang, C. T. Olesen, C. Papon, X. Zhou, L. Midolo, S. Scholz, A. D. Wieck, A. Ludwig, *et al.*, *Science advances* **6**, eabc8268 (2020).
- ¹⁵N. Tomm, A. Javadi, N. O. Antoniadis, D. Najer, M. C. Löbl, A. R. Korsch, R. Schott, S. R. Valentin, A. D. Wieck, A. Ludwig, *et al.*, *Nature Nanotechnology* **16**, 399 (2021).
- ¹⁶B. Kamps, J. Kettler, M. Bock, J. N. Becker, C. Arend, A. Lenhard, S. L. Portalupi, M. Jetter, P. Michler, and C. Becher, *Optics express* **24**, 22250 (2016).
- ¹⁷C. L. Morrison, M. Rambach, Z. X. Koong, F. Graffitti, F. Thorburn, A. K. Kar, Y. Ma, S.-I. Park, J. D. Song, N. G. Stoltz, *et al.*, *Applied Physics Letters* **118**, 174003 (2021).
- ¹⁸B. Da Lio, C. Faurby, X. Zhou, M. L. Chan, R. Uppu, H. Thyrrstrup, S. Scholz, A. D. Wieck, A. Ludwig, P. Lodahl, *et al.*, *Advanced Quantum Technologies* **5**, 2200006 (2022).
- ¹⁹E. Semenova, R. Hosten, G. Patriarache, O. Mauguin, L. Largeau, I. Robert-Philip, A. Beveratos, and A. Lemaître, *Journal of Applied Physics* **103**, 103533 (2008).
- ²⁰L. Seravalli, G. Trevisi, P. Frigeri, D. Rivas, G. Munoz-Matutano, I. Suarez, B. Alén, J. Canet-Ferrer, and J. P. Martínez-Pastor, *Applied Physics Letters* **98**, 173112 (2011).
- ²¹S. L. Portalupi, M. Jetter, and P. Michler, *Semiconductor Science and Technology* **34**, 053001 (2019).
- ²²K. D. Zeuner, K. D. Jöns, L. Schweickert, C. Reuterskiöld Hedlund, C. Nuñez Lobato, T. Lettner, K. Wang, S. Gyger, E. Scholl, S. Steinhauer, *et al.*, *ACS photonics* **8**, 2337 (2021).
- ²³A. Barbiero, J. Huwer, J. Skiba-Szymanska, D. J. Ellis, R. M. Stevenson, T. Müller, G. Shooter, L. E. Goff, D. A. Ritchie, and A. J. Shields, *ACS Photonics* **9**, 3060 (2022).
- ²⁴C. Nawrath, R. Joos, S. Kolatschek, S. Bauer, P. Pruy, F. Hornung, J. Fischer, J. Huang, P. Vijayan, R. Sittig, *et al.*, arXiv preprint arXiv:2207.12898 (2022).
- ²⁵C. Nawrath, H. Vural, J. Fischer, R. Schaber, S. Portalupi, M. Jetter, and P. Michler, *Applied Physics Letters* **118**, 244002 (2021).
- ²⁶T. Miyazawa, K. Takemoto, Y. Sakuma, S. Hirose, T. Usuki, N. Yokoyama, M. Takatsu, and Y. Arakawa, *Japanese Journal of Applied Physics* **44**, L620 (2005).
- ²⁷M. D. Birowosuto, H. Sumikura, S. Matsuo, H. Taniyama, P. J. van Veldhoven, R. Nötzel, and M. Notomi, *Scientific reports* **2**, 321 (2012).
- ²⁸M. Benyoucef, M. Yacob, J. Reithmaier, J. Kettler, and P. Michler, *Applied Physics Letters* **103**, 162101 (2013).
- ²⁹T. Miyazawa, K. Takemoto, Y. Nambu, S. Miki, T. Yamashita, H. Terai, M. Fujiwara, M. Sasaki, Y. Sakuma, M. Takatsu, *et al.*, *Applied Physics Letters* **109**, 132106 (2016).
- ³⁰T. Müller, J. Skiba-Szymanska, A. Krysa, J. Huwer, M. Felle, M. Anderson, R. Stevenson, J. Heffernan, D. A. Ritchie, and A. Shields, *Nature communications* **9**, 862 (2018).
- ³¹A. Musiał, M. Mikulicz, P. Mrowiński, A. Zielińska, P. Sitarek, P. Wyborski, M. Kuniej, J. Reithmaier, G. Sęk, and M. Benyoucef, *Applied Physics Letters* **118**, 221101 (2021).
- ³²M. Anderson, T. Müller, J. Skiba-Szymanska, A. Krysa, J. Huwer, R. Stevenson, J. Heffernan, D. Ritchie, and A. Shields, *Applied Physics Letters* **118**, 014003 (2021).
- ³³P. Holewa, A. Sakanas, U. M. Gür, P. Mrowiński, A. Huck, B.-Y. Wang, A. Musiał, K. Yvind, N. Gregersen, M. Syperek, *et al.*, *ACS photonics* **9**, 2273 (2022).
- ³⁴P. Holewa, E. Zięba-Ostój, D. A. Vajner, M. Wasiluk, B. Gaál, A. Sakanas, M. Burakowski, P. Mrowiński, B. Krajnik, M. Xiong, *et al.*, arXiv preprint arXiv:2304.02515 (2023).
- ³⁵Y. Berdnikov, P. Holewa, S. Kadkhodazadeh, J. M. Smigiel, A. Frackowiak, A. Sakanas, K. Yvind, M. Syperek, and E. Semenova, arXiv preprint arXiv:2301.11008 (2023).
- ³⁶H. Jayakumar, A. Predojević, T. Huber, T. Kauten, G. S. Solomon, and G. Weihs, *Physical review letters* **110**, 135505 (2013).
- ³⁷M. Reindl, D. Huber, C. Schimpf, S. F. C. da Silva, M. B. Rota, H. Huang, V. Zwiller, K. D. Jöns, A. Rastelli, and R. Trotta, *Science Advances* **4**, eaau1255 (2018).
- ³⁸C. Nawrath, F. Olbrich, M. Paul, S. Portalupi, M. Jetter, and P. Michler, *Applied Physics Letters* **115**, 023103 (2019).
- ³⁹G. A. Narvaez, G. Bester, A. Franceschetti, and A. Zunger, *Physical Review B* **74**, 205422 (2006).
- ⁴⁰E. Schöll, L. Schweickert, L. Hanschke, K. D. Zeuner, F. Sbresny, T. Lettner, R. Trivedi, M. Reindl, S. F. C. Da Silva, R. Trotta, *et al.*, *Physical Review Letters* **125**, 233605 (2020).
- ⁴¹D. Bauch, D. Siebert, K. D. Jöns, J. Förstner, and S. Schumacher, arXiv preprint arXiv:2303.13871 (2023).
- ⁴²C.-K. Hong, Z.-Y. Ou, and L. Mandel, *Physical review letters* **59**, 2044 (1987).
- ⁴³A. Thoma, P. Schnauber, M. Gschrey, M. Seifried, J. Wolters, J.-H. Schulze, A. Strittmatter, S. Rodt, A. Carmele, A. Knorr, *et al.*, *Physical review letters* **116**, 033601 (2016).
- ⁴⁴D. Huber, M. Reindl, J. Aberl, A. Rastelli, and R. Trotta, *Journal of Optics* **20**, 073002 (2018).
- ⁴⁵F. Sbresny, L. Hanschke, E. Schöll, W. Rauhaus, B. Scaparra, K. Boos, E. Z. Casalengua, H. Riedl, E. Del Valle, J. J. Finley, *et al.*, *Phys. Rev. Lett.* **128**, 093603 (2022).
- ⁴⁶J. Yan, S. Liu, X. Lin, Y. Ye, J. Yu, L. Wang, Y. Yu, Y. Zhao, Y. Meng, X. Hu, *et al.*, *Nano Lett.* **22**, 1483 (2022).
- ⁴⁷Y. Wei, S. Liu, X. Li, Y. Yu, X. Su, S. Li, X. Shang, H. Liu, H. Hao, H. Ni, S. Yu, Z. Niu, J. Iles-Smith, J. Liu, and X. Wang, *Nat. Nanotechnol.* **17**, 470 (2022), 2109.09284.
- ⁴⁸M. Bozzio, M. Vyvlecka, M. Cosacchi, C. Nawrath, T. Seidelmann, J. C. Loredó, S. L. Portalupi, V. M. Axt, P. Michler, and P. Walther, *npj Quantum Information* **8**, 104 (2022).
- ⁴⁹Y. Karli, D. A. Vajner, F. Kappe, P. C. Hagen, L. M. Hansen, R. Schwarz, T. K. Bracht, C. Schimpf, S. F. C. da Silva, P. Walther, *et al.*, arXiv preprint arXiv:2305.20017 (2023).